NeuroImage: Clinical 10 (2016) 129–139

Contents lists available at ScienceDirect

NeuroImage: Clinical

journal homepage: www.elsevier.com/locate/ynicl

Frontoparietal white matter integrity predicts haptic performance in chronic stroke

Alexandra L. Borstad[a,*], Seongjin Choi[b], Petra Schmalbrock[c], Deborah S. Nichols-Larsen[d]

[a]Division of Physical Therapy, The Ohio State University, School of Health and Rehabilitation Science, 453 W. 10th Avenue, Columbus, OH 43210, United States
[b]National Institute on Aging, Harbor Hospital, Baltimore, MD, United States
[c]Department of Radiology, College of Medicine, The Ohio State University, Columbus, OH, United States
[d]School of Health and Rehabilitation Sciences, The Ohio State University, Columbus, OH, United States

ARTICLE INFO

Article history:
Received 16 July 2015
Received in revised form 6 November 2015
Accepted 11 November 2015
Available online 12 November 2015

Keywords:
Haptic performance
Stroke
Upper extremity
Diffusion MRI
Probabilistic tractography
Hand Active Sensation Test
Sensorimotor
Frontoparietal network

ABSTRACT

Frontoparietal white matter supports information transfer between brain areas involved in complex haptic tasks such as somatosensory discrimination. The purpose of this study was to gain an understanding of the relationship between microstructural integrity of frontoparietal network white matter and haptic performance in persons with chronic stroke and to compare frontoparietal network integrity in participants with stroke and age matched control participants. Nineteen individuals with stroke and 16 controls participated. Haptic performance was quantified using the Hand Active Sensation Test (HASTe), an 18-item match-to-sample test of weight and texture discrimination. Three tesla MRI was used to obtain diffusion-weighted and high-resolution anatomical images of the whole brain. Probabilistic tractography was used to define 10 frontoparietal tracts total; Four intrahemispheric tracts measured bilaterally 1) thalamus to primary somatosensory cortex (T–S1), 2) thalamus to primary motor cortex (T–M1), 3) primary to secondary somatosensory cortex (S1 to SII) and 4) primary somatosensory cortex to middle frontal gyrus (S1 to MFG) and, 2 interhemispheric tracts; S1–S1 and precuneus interhemispheric. A control tract outside the network, the cuneus interhemispheric tract, was also examined. The diffusion metrics fractional anisotropy (FA), mean diffusivity (MD), axial (AD) and radial diffusivity (RD) were quantified for each tract. Diminished FA and elevated MD values are associated with poorer white matter integrity in chronic stroke. Nine of 10 tracts quantified in the frontoparietal network had diminished structural integrity poststroke compared to the controls. The precuneus interhemispheric tract was not significantly different between groups. Principle component analysis across all frontoparietal white matter tract MD values indicated a single factor explained 47% and 57% of the variance in tract mean diffusivity in stroke and control groups respectively. Age strongly correlated with the shared variance across tracts in the control, but not in the poststroke participants. A moderate to good relationship was found between ipsilesional T–M1 MD and affected hand HASTe score ($r = -0.62$, $p = 0.006$) and less affected hand HASTe score ($r = -0.53$, $p = 0.022$). Regression analysis revealed approximately 90% of the variance in affected hand HASTe score was predicted by the white matter integrity in the frontoparietal network (as indexed by MD) in poststroke participants while 87% of the variance in HASTe score was predicted in control participants. This study demonstrates the importance of frontoparietal white matter in mediating haptic performance and specifically identifies that T–M1 and precuneus interhemispheric tracts may be appropriate targets for piloting rehabilitation interventions, such as noninvasive brain stimulation, when the goal is to improve poststroke haptic performance.

1. Introduction

Active sensation or haptic touch is the ability to use movement of the hand and arm to solicit somatosensory information from the environment (Lederman and Klatzky, 1997). Haptic impairment is a common result of stroke identified in 31–89% of cases (Kim and Choi-Kwon, 1996; Gaubert and Mockett, 2000; Connell et al., 2008; Carey and Matyas, 2011; Borstad et al., 2012a). The functional consequence of haptic impairment can be conceptualized in two ways. First, there is the loss of the hand's natural role as the primary somatosensory receptor of the environment (Lederman and Klatzky, 1998). Second, there is reduced somatosensory afferent information that is particularly important for

* Corresponding author.
E-mail addresses: Borstad.2@osu.edu (A.L. Borstad), seongjin.choi@nih.gov (S. Choi), Schmalbrock.1@osu.edu (P. Schmalbrock), Larsen.64@osu.edu (D.S. Nichols-Larsen).

http://dx.doi.org/10.1016/j.nicl.2015.11.007

dexterous movements (Classen et al., 2000). Hence, haptics and manual dexterity are co-dependent aspects of sensorimotor performance.

Stroke mainly affects subcortical structures and white matter (Corbetta et al., 2015). Several studies in stroke describe the relationship between white matter integrity and poststroke motor performance; however, the extent to which the integrity of white matter within the frontoparietal network is related to haptic performance is largely unknown. Constituent regions of the frontoparietal network associated with haptic performance have been identified using functional MRI; they are widely distributed and include primary and secondary somatosensory cortices, the premotor cortex, the posterior parietal cortex and the cerebellum (Stoeckel et al., 2003; Harada et al., 2004; Carey et al., 2011; Borstad et al., 2012a; Van de Winckel et al., 2005, 2012). Efficient information processing between brain areas is requisite to function and dependent upon the integrity of their white matter connections (Seidl, 2014). Because stroke results in diminished integrity both local to and distant from the lesion (Crofts et al., 2011; Borich et al., 2012; Auriat et al., 2015; Lindberg et al., 2007, 2011; Yin et al., 2013; Lim et al., 2012; Carter et al., 2012), diminished integrity in the distributed network that supports somatosensation may explain, in part, why somatosensation was found to be impaired in both the affected and less affected upper extremity after stroke (Borstad et al., 2012a; Kim and Choi-Kwon, 1996; Connell et al., 2008; Carey and Matyas, 2011). Parts of the frontoparietal network have been examined in chronic stroke for their relationship to sensorimotor performance. In a previous study we found that integrity of the sensory aspect of the superior thalamic radiation, which includes all afferent connections to S1 (Wakana et al., 2004), was related to haptic performance (Borstad et al., 2012a). Buch and colleagues showed the structural connectivity in the superior longitudinal fascicles II and III between frontal and parietal regions were associated with better sensorimotor rhythm modulation skill in severe chronic hemiparesis (Buch et al., 2012). Borich and colleagues reported integrity of the sensory region of the CC was reduced following chronic stroke but was not correlated with manual dexterity as measured by the Box and Blocks Test. A somatosensory measure was not included in their assessment (Borich et al., 2012).

Quantitative diffusion tensor imaging (DTI) allows calculation and visualization of parameters that are sensitive to intrinsic features of brain tissue at the macromolecular, cellular, and tissue level, similar to histological stains; thus, DTI parameters are said to reflect tissue microstructural integrity (Basser and Pierpaoli, 1996). The two most frequently used diffusion metrics are fractional anisotropy (FA) and mean diffusivity (MD) (Vos et al., 2012). FA quantifies the degree of directional dependence of diffusion while MD reflects the overall amount of isotropic diffusion. The diffusion signal can be further reduced to individual components that include: axial diffusivity (AD) largest eigenvalue, presumed to be along the length of the axons and radial diffusivity (RD) refers to the average of the next two smaller eigenvalues, which are presumed to be perpendicular to the axon. Elevated MD and diminished FA are associated with poorer white matter microstructural integrity in chronic stroke (Schlaug et al., 1997).

Because there is limited knowledge of the extent to which stroke affects white matter structural integrity in the distributed frontoparietal network, in the present study, we compared frontoparietal network microstructural integrity in participants with stroke to age-matched control participants. We also examined the extent to which frontoparietal network microstructural integrity related to haptic performance as measured by the Hand Active Sensation Test (HASTe) (Borstad et al., 2015; Williams et al., 2006). The goals were to 1) identify frontoparietal network tracts in which poststroke participants had diminished integrity compared to controls and 2) determine if the microstructural integrity of frontoparietal tracts was related to haptic performance. We hypothesized that there would be significant differences between poststroke and control participants in frontoparietal tract integrity and that diminished tract integrity would correlate with haptic performance of the stroke affected upper extremity.

2. Methods

2.1. Subjects

Nineteen individuals with stroke and sixteen age-matched controls participated. Inclusion criteria: a single stroke (ischemic or hemorrhagic) diagnosed greater than 3 months prior to enrollment, 10° of active finger extension in the affected hand (required to complete haptic testing), communication in English sufficient to provide informed consent and follow study instructions. Exclusion criteria: Mini Mental Status Exam score ≤24, severe spatial or visual neglect (a positive Albert's Test), apraxia or hemianopsia (informal assessment during screening), other diagnosed neurologic or sensory disorder, claustrophobia, and ferrous implants. Control participants met the criteria when they had no history of stroke or other neurologic condition, and no focal abnormality on MRI. The University Biomedical Sciences Institutional Review Board approved this study and written informed consent was obtained prior to participation.

2.2. Clinical evaluation

Haptic performance was quantified using the Hand Active Sensation Test (HASTe), an 18-trial test of weight and texture discrimination, valid and reliable for measurement of haptic performance in healthy individuals and persons poststroke (Williams et al., 2006; Borstad et al., 2015). To complete the test, for each trial, participants manually explore one test object and three sample objects that vary by weight or texture without using vision. Participants are asked to indicate which sample object is a match to the test object without discussing the properties of the objects. The accuracy score out of 18 is recorded for each hand; 13 or greater out of 18 possible has been considered the cut off for normal performance (Williams et al., 2006). Because of the match-to-sample design 6/18 could be considered a chance score. HASTe scores for control and poststroke participants were normally distributed and are reported in Table 1. The 6-item Wolf Motor function Test was used to quantify motor performance (Bogard et al., 2009). The 6 items included: hand to table (front), hand to box (front), reach and retrieve, lift can, lift pencil, and fold towel. Pre-stroke handedness was determined using the Edinburgh inventory (Oldfield, 1971). Clinical evaluation and MRI took place on the same day for each participant. Demographic, neurologic, and sensory descriptors are given in Table 1.

2.3. MRI acquisition

A 3 Tesla MR scanner (Philips, Best, The Netherlands) with a body transmit and 8-channel receiver coil was used. High-resolution 3D T1-weighted Magnetization Prepared Rapid Acquired Gradient Echo (MRRAGE) anatomical images with an isotropic voxel size of 1 mm^3 were acquired for spatial normalization to a standard atlas. T2 weighted Fluid Attenuated Inversion Recovery (FLAIR) images were acquired in the axial plane with a voxel size of $2 \times 2.5 \times 2$ mm for calculation of lesion volume. Diffusion-weighted images were acquired in the axial plane with parameters: TR/TE = 9750/92 ms, FOV = 256×256 mm^2, Matrix = 128×128, isotropic voxel size 2 mm^3, gap = 0.0 mm, two b-values 0 and 1000 s/mm^2, diffusion-weighting gradient directions = 32, SENSE reduction factor of 2.2, scan time of 6 min. The signal-to-noise ratio (SNR, 25.6 for the entire white matter region) was calculated from a representative control participant. SNR with sensitivity encoding (SENSE) reconstruction was determined from a minimally diffusion-weighted image ($b = 0$ s/mm^2) and a noise image with radio frequency field off (Choi et al., 2011).

2.4. Lesion analysis

Two different methods were used to characterize the stroke lesions in participants. First, for visualization purposes only lesion masks were

Table 1
Clinical details of participants.

ID	Age	Sex	Dom. hand	More affected hand	Chronicity (months)	HASTe (less affected/more affected)	6-item Wolf (rate/60s)	Lesion volume (cm^3)	Brain volume (cm^3)
Poststroke									
002	75	M	R	L	12	7/8	22.5	14.3	1424
003	62	F	R	R	9	15/14	27.9	2.1	1459
004	55	F	R	L	24	10/7	27.3	20.1	1393
005	46	F	R	R	96	10/4	38.7	9.9	1394
007	30	M	R	L	60	16/12	23.1	37.5	1390
008	84	F	R	R	11	8/13	26.1	0.6	1356
009	71	M	R	R	10	12/11	41.1	1.9	1431
011	64	M	R	R	20	11/10	19.8	2.6	1344
012	62	M	R	L	16	9/11	35.6	8.0	1320
013	39	F	L	R	4	12/8	18.3	3.9	1438
014	61	F	R	L	24	13/13	33.9	6.0	1298
015	77	F	R	R	8	8/9	41.9	1.3	1376
016	70	M	R	L	21	14/15	53.9	.87	1346
017	60	F	R	L	94	8/6	23.0	110.1	1454
018	85	F	R	L	38	13/9	42.8	.056	1269
019	65	M	R	L	41	10/7	24.2	3.35	1471
020	71	F	R	L	8	10/7	38.5	49.4	1350
021	69	M	R	R	9	10/10	2.0	54.3	1402
022	48	F	R	R	13	16/13	27.0	4.1	1412
Mean	62.8	8M/11F	18R/1L	9R/10L	13 (24)	11.5/9.9 (R/L)	29.9 (11.6)	17.4 (27.9)	1386
Control									
A	53	F	L	NA	NA	12/12	NT	NA	1394
B	38	F	L			16/16			1522
C	41	F	R			14/11			1498
D	72	M	R			10/10			1432
E	85	F	R			11/7			1391
F	60	F	R			12/11			1481
G	69	M	R			8/8			1387
H	64	M	R			13/13			1113
I	58	F	R			16/14			1500
J	63	M	R			11/11			1475
K	69	F	R			16/16			1463
L	47	F	R			14/17			1518
M	68	M	R			9/12			1347
N	74	F	R			12/13			1279
O	40	M	R			1215			1476
P	46	M	R			16/14			1379
Mean	59.2	7M/9F	14R/2L			12.6/12.5			1432
T-test	$p = 0.45$					$p = 0.11/p = 0.01$			$p = 0.33$

NA, not applicable; Dom., dominant, R, right; L, left; NT, not tested; t-test, two-tailed t-test; HASTe, Hand Active Sensation Test; the majority of participants were right hand so HASTe scores from the less affected upper extremity of the poststroke participants were compared to the right hand of the control participants, scores from the more affected upper extremity were compared to the left hand of control participants.

created by manually drawing the lesion in the individuals T1-weighted image (Fig. 1) (Rorden and Brett, 2000). For quantification, stroke lesion volume was determined from T2 weighted FLAIR images by manually outlining signal abnormality slice-by slice in the axial plane (Bazin et al., 2007; Orrison, 2008).

2.5. Brain volume measurement

Gray and white matter volumes were calculated using each participant's T1 image. Stroke lesions were nulled to prevent misclassification of voxels prior to quantification; therefore, nulled voxels are not included in the regional or normalized brain volumes. All participant images were oriented, cropped to exclude non-brain/skull data (Smith, 2002) and analyzed using SIENAX version 2.6 (Smith et al., 2001, 2002). Next, affine registration was used to register the brain image to standard space (Montreal Neurologic Institute 152) (Jenkinson et al., 2002; Jenkinson and Smith, 2001). Skull dimensions were used to determine the registration scaling in order to normalize brain volume to head size. Tissue-type segmentation was carried out with partial volume estimation in order to quantify brain volume (gray matter + white matter) (Zhang et al., 2001), with >99% accuracy (Smith et al., 2002). Visual inspection of whole brain segmentation verified results.

2.6. Diffusion tensor imaging

The following objective approach was used to delineate tracts of interest in this study. Diffusion tensor image analysis was performed using FMRIB Diffusion Toolbox (FDT) included in Functional MRI of the Brain Software Library (FSL) (Analysis Group, FMRIB, Oxford, UK) (Smith et al., 2004). Image artifacts due to eddy currents and bulk head motion were minimized including b-matrix rotation during motion correction (Smith et al., 2004). Non-brain tissue was removed (Smith et al., 2002). Scalar maps for mean tract FA, MD, AD and RD were generated. Because the component diffusion metrics may provide more specific information about the underling tissue properties they were included in our analysis (Budde et al., 2007; Song et al., 2003). For poststroke participants, high-resolution anatomical images were masked to null voxels in the region of their lesion to minimize lesion related structural changes from affecting the registration. Affine (12 degrees-of-freedom) registration was used to obtain transformation matrices first between the diffusion and anatomical space and then between the anatomical and standard space (Montreal Neurologic

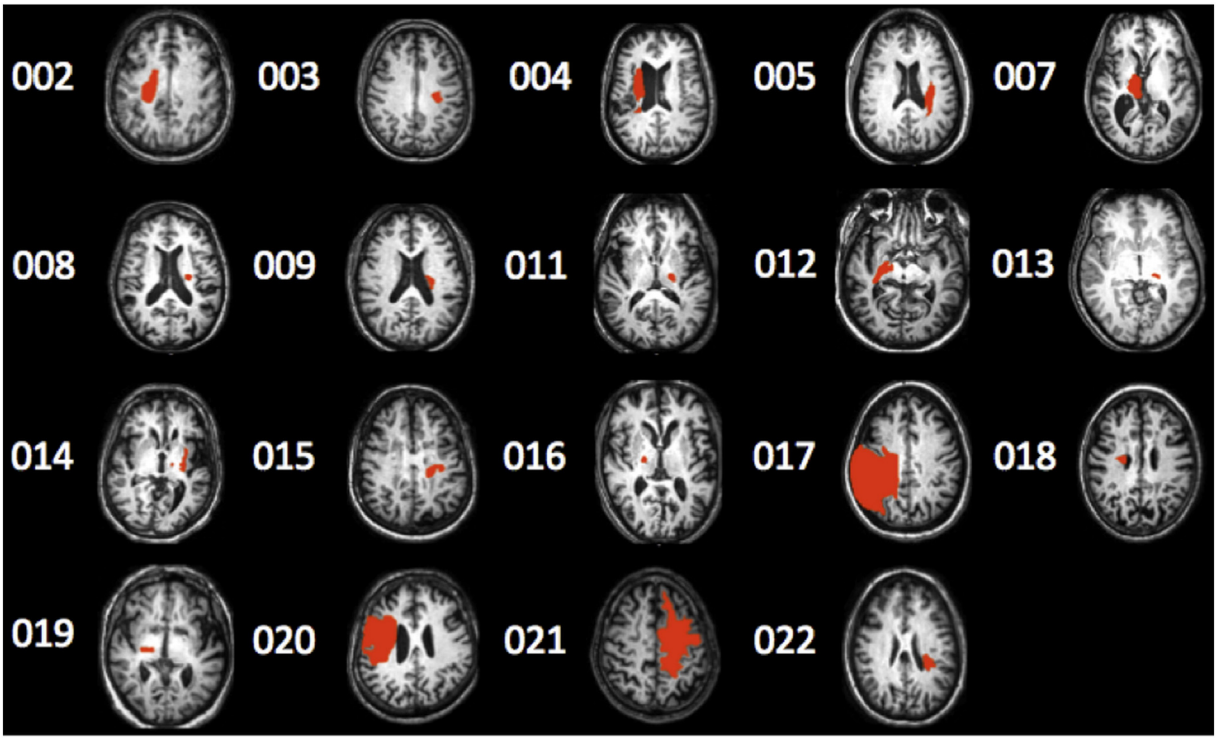

Fig. 1. Lesion in poststroke participants on T1 image (radiologic convention). The axial slice of with the largest lesion volume is shown.

Institute 152) (Jenkinson and Smith, 2001). Binarized white matter masks (Zhang et al., 2001) were realigned into diffusion space and used to constrain probabilistic tracking.

Based on previous fMRI studies (Harada et al., 2004; Borstad et al., 2012a; Carey et al., 2011; Tunik et al., 2007), 10 white matter tracts of interest in the somatosensory discrimination network were identified;

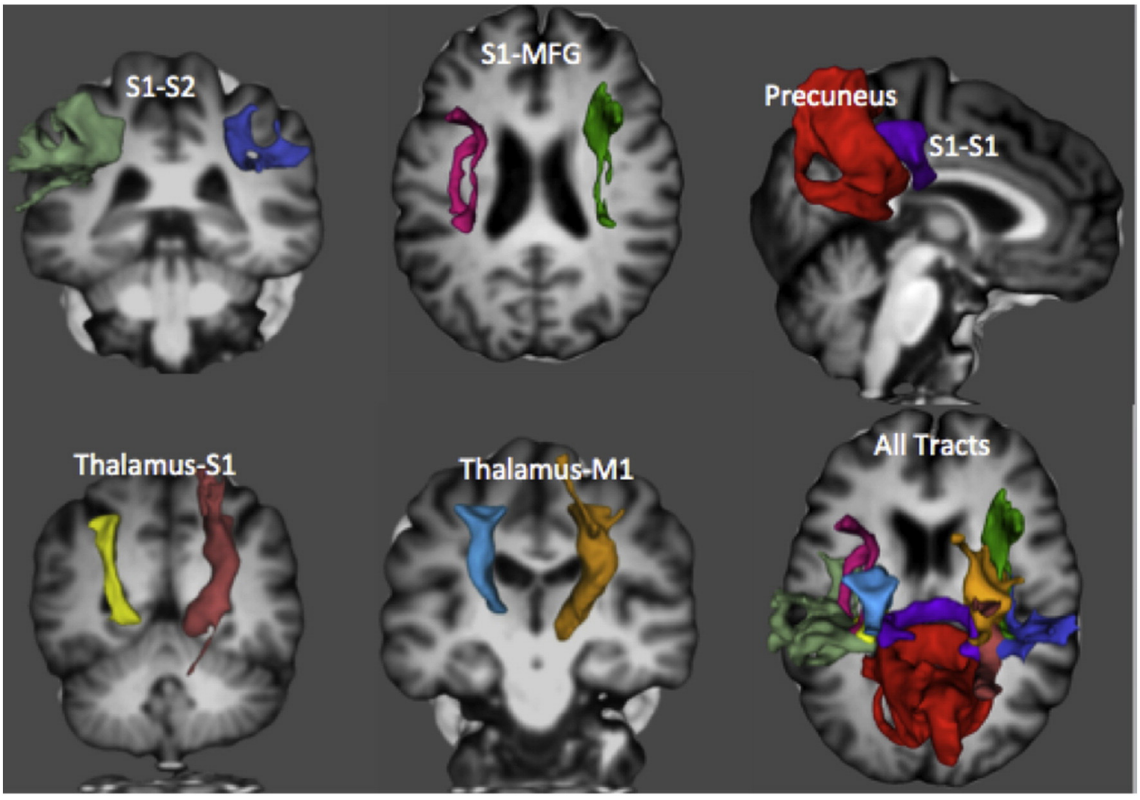

Fig. 2. Example 3D renderings of frontoparietal network tracts generated using probabilistic tractography. Four intrahemispheric (S1 to S2, thalamus to S1, S1 to MFG and thalamus to M1) measured bilaterally and, 2 interhemispheric tracts (S1–S1 and precuneus interhemispheric) were modeled. A control tract outside the network, the cuneus interhemispheric is not shown. Descriptions of the standard space seed, target, exclusion and termination masks can be found in the Appendix.

2 were interhemispheric and 4 were intrahemispheric (Fig. 2). The interhemispheric tracts were: S1 to S1, and Precuneus interhemispheric. The intrahemispheric tracts measured in both hemispheres were thalamus to primary somatosensory cortex (S1), thalamus to primary motor cortex (M1), S1 to middle frontal gyrus (MFG), S1 to secondary somatosensory cortex (SII). Previously the T-S1 tract was related to poststroke haptic performance, it includes all sensory afferents to the S1 cortex (Borstad et al., 2012a). Thalamus to M1 includes efferent pathways from the frontoparietal network. These 10 tracts were successfully modeled with probabilistic tractography using a two-ROI approach (Heiervang et al., 2006). A minimum FA threshold of 0.2 was used to constrain probabilistic tracking. Our attempt to model a tract between left S1 and right SII (and right S1 and left SII) was unsuccessful in a series of 5 control subjects so was discontinued. We hypothesize this was due to the accumulation of uncertainty in the probabilistic algorithm caused by distance and curves in the tracts (Jbabdi and Johansen-Berg, 2011). To establish that the adjacent thalamocortical tracts studied here were independent (set a priori at <10% overlap), the extent of overlap was calculated in each participant. The mean amount of overlap in voxels in stroke and control participants was 7.76% and 7.88% respectively. To provide a basis for comparison to frontoparietal network tracts studied here we also quantified the interhemispheric tract between right and left cuneus cortices. Circulation for the cuneus cortex comes from the posterior cerebral artery. As no participants in this study had posterior cerebral artery distribution stroke this tract was selected for control-comparison purposes. Standard space masks used for probabilistic tracking met reproducible criteria (and are detailed in Supporting Information-end of this document). The position of tracts of interest was confirmed visually in each participant. As indices of tract integrity, mean tract FA, MD, AD and RD were then calculated. All voxels through which a probabilistic streamline passed were used to calculate means.

2.7. Statistics

Differences between the stroke and control group for HASTe score, brain volume, and age were determined using the two-sample t-test; p-Values ≤ 0.05 were considered significant (Table 1). Because our stroke an control groups were closely matched for handedness, to determine the effect of group (control, right hemisphere stroke, left hemisphere stroke) for each tract, we decided to compare right and left hemispheres directly, rather than comparing lesioned hemisphere to non-dominant hemisphere, two-sample t-tests were used for this comparison. The results were corrected for multiple comparisons using false discovery rate (FDR) correction (Benjamini and Hochberg, 1995). Corrected p-values were considered statistically significant at p ≤ 0.03 (Table 2).

Fractional anisotropy and mean diffusivity are known to reflect white matter integrity following stroke. Of the two metrics, in our data, MD had the lowest coefficient of variation across the 10 frontoparietal network tracts we quantified in both the poststroke and control groups, therefore it was used for the following three analyses: 1) to explain frontoparietal network variance principal components' analysis (PCA) was conducted on the correlations across the 10-frontoparietal tract mean MD values (Table 3). 2) To evaluate the relationship between haptic performance of the affected hand and network integrity we examined the relationship between ipsilesional and interhemispheric tract MD and HASTe scores using Pearson correlation coefficient. Bonferroni correction for 6 comparisons resulted in an adjusted alpha of $p < 0.008$ (Table 3). 3) To evaluate how well frontoparietal white matter integrity and other variables (age, brain volume and lesion volume) predicted HASTe scores of the affected and less affected hand we used forward stepwise multiple regression. Statistical analyses were performed in JMP® Pro 11.0.0. These data have been made publically available, to request access please contact the corresponding author.

3. Results

3.1. Haptic performance

HASTe scores for both hands of all participants are shown in Table 1. Poststroke participants exhibited a wide range of haptic ability. HASTe scores ranged from 4 to 16 for the right hand and 6 to 16 for the left hand and were normally distributed. A moderate to good correlation was identified between less affected and more affected hand HASTe scores ($r = 0.58$, $p = 0.009$). Control participants also exhibited a range of haptic ability. Scores ranged from 8 to 16 for the right hand and 7 to 16 for the left hand. Control participant right and left hand HASTe scores were also correlated ($r = 0.72$, $p = 0.001$). There was a significant difference between stroke and control group means on the HASTe for comparison between the more affected hand of poststroke participants and the left hand of controls ($p = 0.01$) (Table 1).

3.2. Brain lesion volume

Gray, white and total brain volumes were not statistically different between groups. Average brain volume for poststroke/control participants was 1386/1415 cm^3. The average cerebral spinal fluid, gray, and white matter volumes for poststroke/control participants were 27/26 cm^3, 703/722 cm^3, and 675/693 cm^3 respectively.

Stroke lesion volume was 17.4 cm^3 on average. Mean (SD) lesion volume for left hemisphere participants ($n = 9$) was 8.9 (17) cm^3, for right hemisphere stroke participants ($n = 10$) was 24.9 (34) cm^3, they were not statistically different ($p = 0.21$). A lesion plot is shown in Fig. 1.

3.3. Tract quantification

Eleven tracts in 35 participants for a total of 385 tracts were modeled. Probabilistic tracts were not established in 37 instances (10%), similar to recent probabilistic tractography studies reporting 11% (De Weijer et al., 2010) and 18% (Yang et al., 2009) error rates. These 'missing' tracts were divided into two categories: 1) biological, in which visible white matter changes (stroke lesion in tract, white matter disease or corpus callosum thinning) were evident; 2) technical, in which no structural explanation was evident. The technical error rate was 6% for controls and 5% for strokes. The biological error rate was 0.5% for controls and 7% for strokes. As different causes resulted in missing tracts, no single method of data imputation could be applied; therefore, only tracts that could be established were included in the analysis. The number of tracts analyzed for each group is given in Table 2.

The right hemisphere stroke group differed from controls on at least one diffusion metric in 8 of 10 tracts in the network. The left hemisphere poststroke differed from controls in 7 of 10 tracts in the network. Neither group differed from controls for the precuneus interhemispheric. Both groups differed from controls for the cuneus interhemispheric (control) tract AD but not MD or FA (Table 2).

To explain frontoparietal network variance we used principal component analyses (PCA) across all 10 white matter tracts for mean MD. PCA was run separately for stroke and control groups. In the control group the PCA results indicated a clear one-factor solution, with the first principal component (PC1) explaining 57% of the variance (Table 3).

In controls, age was strongly correlated with PC1 ($r = 0.95$, $p < 0.0001$) (Fig. 3a). For the stroke group PC1 explained 47% of the variance. Unlike the controls, PC1 for the poststroke participants did not have a statistically significant correlation with age ($r = 0.20$, $p = 0.42$) (Fig. 3b). We then examined other factors for correlation with PC1 in the poststroke group. Brain volume was not correlated ($r = 0.13$, $p = 0.59$), chronicity ($r = 0.42$, $p = 0.07$) and lesion volume ($r = 0.41$, $p = 0.07$) had fair relationships at trend level of significance.

Table 2
Comparison of tract diffusion metrics by group.

Measures	Control		R stroke		L stroke		Control vs. R stroke		Control vs. L stroke	
	Mean	CV	Mean	CV	Mean	CV	*t*	p	*t*	p
R T-S1	$n = 15$		$n = 9$		$n = 9$					
FA	0.45	6.9	0.38	19.7	0.43	8.2	**3.05**	**0.0059**	1.13	0.2726
MD	7.8	7.0	10.1	22.1	8.4	11.4	**3.84**	**0.0009**	2.19	0.0391
AD	11.7	11.7	13.9	14.3	12.4	8.5	**4.13**	**0.0004**	2.15	0.0431
RD	5.9	15.7	8.2	29.4	6.5	14.8	**3.11**	**0.0051**	1.19	0.2456
L T-S1	$n = 16$		$n = 8$		$n = 9$					
FA	0.46	6.6	0.43	12.1	0.42	5.9	2.22	0.0363	**3.56**	**0.0019**
MD	7.7	6.7	8.5	10.1	8.8	7.6	**3.07**	**0.0052**	**4.45**	**0.0002**
AD	11.8	5.1	12.5	6.5	12.9	5.8	**2.61**	**0.0154**	**3.85**	**0.0009**
RD	5.7	9.5	6.6	14.6	6.8	9.9	**3.01**	**0.0060**	**4.39**	**0.0003**
R T-M1	$n = 15$		$n = 9$		$n = 9$					
FA	0.45	6.2	0.38	8.3	0.44	9.3	**6.25**	**<.0001**	1.03	0.3119
MD	7.5	7.4	9.5	9.3	8.2	8.3	**6.54**	**<.0001**	**2.45**	**0.0229**
AD	11.4	6.2	13.2	8.3	11.7	14.0	**4.82**	**<.0001**	0.62	0.5416
RD	5.6	9.4	7.6	11.2	6.2	13.3	**7.13**	**<.0001**	**2.32**	**0.0301**
L T-M1	$n = 15$		$n = 9$		$n = 10$					
FA	0.47	7.2	0.44	9.1	0.39	11.7	2.10	0.0468	**5.18**	**<.0001**
MD	7.5	7.8	8.6	8.6	9.1	16.2	**3.38**	**0.0026**	**3.88**	**0.0008**
AD	11.5	5.9	12.8	6.5	12.4	12.1	**3.05**	**0.0056**	**2.80**	**0.0105**
RD	5.5	10.7	6.3	11.7	7.3	20.2	3.25	0.0035	**4.30**	**0.0003**
R S1-SII	$n = 15$		$n = 8$		$n = 9$					
FA	0.38	10.0	0.32	24.5	0.35	6.5	**2.44**	**0.0235**	2.19	0.0399
MD	8.1	5.4	10.1	17.0	8.9	9.7	**4.30**	**0.0003**	**3.20**	**0.0043**
AD	11.1	4.3	13.1	9.3	12.1	7.6	**5.29**	**<.0001**	**2.85**	**0.0096**
RD	6.6	8.1	8.6	23.4	7.4	11.9	**3.78**	**0.0010**	**3.02**	**0.0065**
L S1-SII	$n = 16$		$n = 8$		$n = 9$					
FA	0.38	14.8	0.35	16.9	0.35	17.8	1.40	0.1750	1.23	0.2303
MD	8.0	9.2	8.6	10.5	9.0	15.5	2.10	0.0474	**2.49**	**0.0208**
AD	11.0	5.4	11.6	7.1	12.1	10.8	1.92	0.0672	**2.76**	**0.0114**
RD	6.4	13.8	7.2	14.8	7.5	19.8	1.95	0.0632	2.23	0.0361
R S1-MFG	$n = 14$		$n = 9$		$n = 9$					
FA	0.35	11.8	0.27	9.6	0.35	12.1	**5.11**	**<.0001**	0.35	0.7298
MD	8.5	12.5	10.4	12.6	9.0	10.5	**3.80**	**0.0010**	1.01	0.3211
AD	11.2	11.2	13.0	11.1	12.0	7.1	**3.13**	**0.0051**	1.71	0.1025
RD	7.1	16.2	9.2	11.2	7.5	13.9	**4.00**	**0.0006**	0.71	0.4823
L S1-MFG	$n = 15$		$n = 8$		$n = 9$					
FA	0.36	9.4	0.33	10.3	0.32	10.0	2.11	0.0467	**2.88**	**0.0089**
MD	8.4	9.5	9.2	9.5	9.4	8.8	**2.46**	**0.0222**	**2.92**	**0.0081**
AD	11.2	6.1	12.0	6.7	12.2	6.8	**2.56**	**0.0180**	**3.05**	**0.0060**
RD	7.0	12.6	7.9	11.8	8.2	10.7	**2.37**	**0.0270**	**2.78**	**0.0111**
S1-S1	$n = 15$		$n = 8$		$n = 8$					
FA	0.48	5.9	0.41	17.0	0.45	7.1	**3.40**	**0.0027**	2.02	0.0567
MD	8.4	5.0	10.1	16.1	9.0	9.0	**3.98**	**0.0007**	**2.46**	**0.0225**
AD	13.0	3.6	14.5	9.5	13.7	8.2	**3.76**	**0.0011**	2.09	0.0492
RD	5.9	10.0	7.9	23.0	6.7	10.3	**3.86**	**0.0009**	**2.64**	**0.0154**
Precuneus	$n = 15$		$n = 8$		$n = 8$					
FA	0.40	7.1	0.39	10.8	0.38	10.6	0.93	0.3640	1.31	0.2058
MD	9.1	5.8	9.7	13.0	9.5	8.1	1.54	0.1378	1.60	0.1244
AD	12.9	5.0	13.6	9.5	13.3	7.0	1.70	0.1038	1.23	0.2325
RD	7.1	8.1	7.7	16.7	7.6	10.8	1.33	0.1993	1.53	0.1405
Cuneus	$n = 11$		$n = 5$		$n = 8$					
FA	0.46	9.3	0.47	10.8	0.51	10.5	0.28	0.7852	2.05	0.0598
MD	9.3	5.2	10.0	8.9	9.3	7.7	2.30	0.0342	0.10	0.9275
AD	14.1	3.4	15.2	5.9	15.0	5.9	**3.22**	**0.0050**	**2.55**	**0.0230**
RD	6.8	10.2	7.4	13.7	6.5	13.6	1.51	0.1491	0.93	0.3675

Bold, significant at 5% FDR (corrected p = 0.03); CV, coefficient of variation; FA, fractional anisotropy; MD, mean diffusivity; AD, axial diffusivity; RD, radial diffusivity; MD, AD, RD units: $\times 10^{-4}$ mm.

3.4. Diffusion parameters and haptic performance

To explore the relationship between tract diffusion parameters and haptic performance in the control participants we conducted Pearson's correlations of left and interhemispheric frontoparietal tracts and right hand HASTe score. We chose the right hand, as it was the dominant hand in the majority of participants. After correction for multiple comparisons a moderate to good relationship was found between right HASTe score and Precuneus MD (and AD) and left S1–MFG AD (Table 4).

To explore the relationship between tract diffusion parameters and haptic performance in the poststroke participants we conducted bivariate Pearson's correlations of iplslesional and interhemispheric frontoparietal tracts and affected hand HASTe score (Table 5). After correction for multiple comparisons a moderate to good relationship was found between ipsilesional T-M1 MD (and RD) and affected hand HASTe score ($r = -0.62$, $p = 0.006$) (Fig. 3). Because haptic performance measured by the HASTe requires somatosensory perception and motor manipulation we wished to discern whether the positive relationship between thalamus–M1 integrity and HASTe score was a function of better motor performance in our participants. To do so we completed a post-hoc correlation between thalamus–M1 MD and the 6-item Wolf Motor function Test ($r = 0.08$, $p = 0.92$) and between the 6-item Wolf and HASTe score ($r = 0.14$, $p = 0.57$) and no statistically significant correlation was identified (Fig. 4).

Table 3
Principal components analysis factor loadings by group.

	Stroke	Control
R T-S1 MD	0.83925	0.86289
L T-S1 MD	0.35606	0.74688
R T-M1 MD	0.83581	0.81729
L T-M1 MD	0.22083	0.62672
R S1-SII MD	0.87726	0.63451
L S1-SII MD	0.44177	0.56079
R S1-MFG MD	0.76003	0.81662
L S1-MFG MD	0.54763	0.79244
S1-S1 MD	0.77120	0.82337
Precuneus MD	0.84081	0.62672
Variance explained by PC1	47%	57%
Mean between tract r	0.38	0.50

PC1 = first principal component.

The interpretation of bivariate correlations is limited given they do not account for the possible influence of other variables. Therefore we used forward stepwise multiple regression analysis to evaluate how well frontoparietal network white matter and other variables (age, brain volume and lesion volume) predicted HASTe scores. The combination of ipsilesional T–M1 and T–S1, Precuneus and S1–S1 resulted in the strongest model ($F(4, 6) = 12.08$, $p = 0.004$) for predicting affected hand HASTe scores. The multiple correlation coefficient (r^2) was 0.90, indicating that approximately 90% of the variability in affected hand HASTe score was predicted by the white matter integrity of these four tracts (as indexed by MD). Beta weights for the individual tracts were precuneus ($\beta = 1.1$, $t = 5.9$, $p = 0.001$), S1–S1 ($\beta = 1.0$, $t = 3.5$, $p = 0.01$), and ipsilesional T–S1 ($\beta = 0.9$, $t = 2.8$, $p = 0.03$), and ipsilesional T–M1 ($\beta = 0.74$, $t = 2.2$, $p = 0.06$) indicating that precuneus tract integrity was the most important variable for predicting affected HASTe score. Age, brain volume and lesion volume were not retained in the model. To predict the less affected hand HASTe score, a single tract, the ipsilesional thalamus–M1 MD and age resulted in the strongest model [$F(2, 15) = 4.6$, $p = 0.028$]. The correlation coefficient was 0.38 indicating that approximately 38% of the variance in less affected hand HASTe score was predicted by white matter in the ipsilesional T–M1 tract and age. Beta weights for ipsilesional T–M1 ($\beta = 0.54$, $t = 2.6$, $p = 0.02$) and age ($\beta = 0.30$, $t = 1.5$, $p = 0.15$) indicate ipsilesional T-M1 was most important for predicting HASTe score for the less affected hand.

To predict the right hand HASTe score for the control participants the 4 left intrahemispheric and two interhemispheric tracts resulted in the strongest model ($F(6, 12) = 6.48$, $p = 0.02$). The multiple correlation coefficient was 0.87 indicating that approximately 87% of the variability in right hand HASTe score was predicted by the white matter integrity of these 6 tracts (as indexed by MD). Beta weights for the individual tracts from strongest to weakest were precuneus ($\beta = 1.5$, $t = 4.2$, $p = 0.005$), left S1–SII ($\beta = 1.0$, $t = 3.1$, $p = 0.02$), left T–S1 ($\beta = 0.92$, $t = 2.7$, $p = 0.04$), left T–M1 ($\beta = 0.82$, $t = 2.0$, $p = 0.09$), S1–S1 ($\beta = 0.49$, $t = 2.4$, $p = 0.05$), and left S1–MFG ($\beta = 0.26$, $t = 1.1$, $p = 0.30$). Age and brain volume were not retained in this model.

4. Discussion

This study had three main findings; first, we demonstrated that the microstructural integrity of the frontoparietal network is diminished both ipsilesionally and contralesionally in chronic stroke with a single factor accounting for nearly half of the shared variance across the 10 tracts studied in this network. Second, frontoparietal network integrity predicted nearly 90% of the variance haptic performance in both poststroke and control participants. Third, multivariate regression analysis suggests that the strongest predictor haptic performance in both poststroke and control models was the precuneus interhemispheric tract integrity. The significance of these findings is discussed below.

4.1. Haptic performance is diminished in the affected hand in chronic stroke

Mean HASTe scores for poststroke and control participants were statistically different when comparing the more affected upper extremity to the left upper extremity of controls and were normally distributed enabling analysis of relationship to white matter integrity using parametric statistics. While the HASTe was sensitive to between group differences in this study, it did not perform as reported by Williams and colleagues in that some control participants (50% with the left and 56% with the right hand) studied here scored lower than the suggested cut off of 13/18 correct matches for normal performance. This cut off was suggested based on the fact that in their control sample ($n = 28$, mean age 60 (14) years) no participants scored less than 13/18. The mean/range in age of their participants was similar to ours so this difference seems unlikely to be related to age. A possible cause for the difference is control participant scores is that a different HASTe kit was used for this study. The HASTe is not commercially produced; therefore subtle differences in construction of the test objects could affect scores. Important to the interpretation of the current studies data is that the same test kit, tester and method of administration was used across both participant groups.

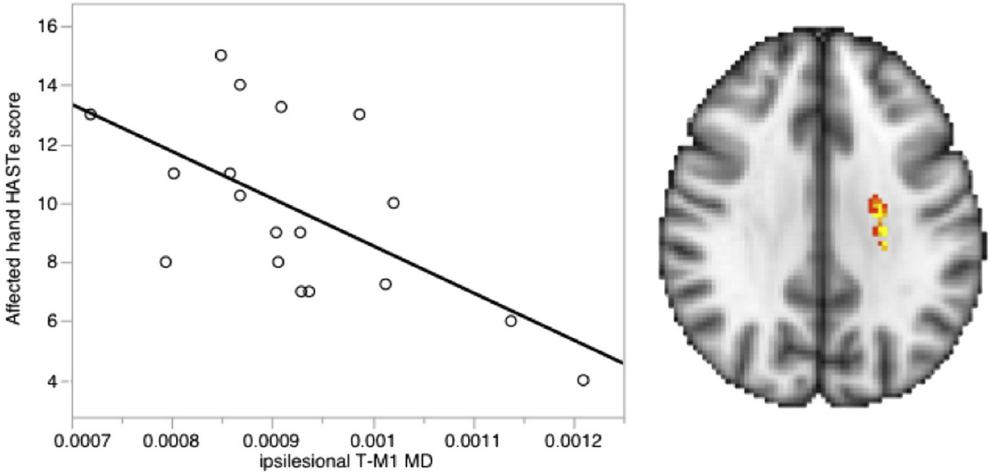

Fig. 3. Thalamocortical white matter mean diffusivity related to haptic performance. One white matter tract in the ipsilesional hemisphere, the thalamus to M1 cortex, had a significant relationship with haptic performance of the affected hand across the poststroke participants ($r = 0.62$, $p = 0.006$). The same tract also had the strongest relationship with less affected hand haptic performance ($r = 0.53$, $p = 0.022$).

Table 4
Pearson's correlation of tract diffusion parameters in control participants by right hand HASTe score.

	Mean FA		Mean MD		Mean AD		Mean RD	
	r	p-Value	r	p-Value	r	p-Value	r	p-Value
Right HASTe								
Left T-S1	0.03	0.907	−0.53	0.036	−0.60	0.014	−0.43	0.097
Left T-M1	0.01	0.953	−0.15	0.592	−0.20	0.469	−0.10	0.711
Left S1-MFG	0.14	0.590	−0.55	0.033	−0.66	0.008*	−0.50	0.060
Left S1-SII	0.27	0.308	−0.08	0.741	−0.46	0.072	−0.03	0.871
S1-S1	0.27	0.324	−0.59	0.018	−0.56	0.031	−0.35	0.195
Precuneus	0.05	0.846	−0.68	0.005*	−0.72	0.002*	−0.53	0.042

With Bonferroni correction p-values are considered significant at p ≤ 0.008. Statistically significant correlations are indicated by an *.

4.2. Microstructural integrity of frontoparietal network white matter is diminished in chronic stroke

Nine of 10 tracts quantified in the frontoparietal network had diminished integrity poststroke compared to the controls as evidenced by diminished FA or increased MD, AD or RD. Only the precuneus interhemispheric tract was not significantly different between groups. The cuneus interhemispheric tract, chosen as a control tract, was also not statistically different between groups for FA or MD, though it was different for AD. These results are consistent with and extend findings from other diffusion imaging studies that have shown that poststroke microstructure is diminished in ipsilesional and contralesional CST (Schaechter et al., 2009), in areas surrounding the lesions and homologous locations in the contralesional hemisphere (Crofts et al., 2011). By quantifying stroke–control variations in white matter integrity the science is progressing toward an understanding of the biological processes, which follow stroke and are associated with recovery (Johansen-Berg and Behrens, 2009). Mechanisms associated with increases in diffusivity local to the lesion include axonal degeneration and gliosis (Pierpaoli et al., 1996; Werring et al., 2000); less frequently reported contralesional hemisphere changes have been referred to as transhemispheric diaschisis (Andrews, 1991).

White matter disturbances occur with aging (Kohama et al., 2012). In particular prefrontal and PLIC areas have been shown to have age-related degeneration (Salat et al., 2005). In our control data, age was strongly correlated with the shared variance in white matter integrity across frontoparietal tracts ($r = 0.95$, $p < 0.0001$). Conversely, the shared variance in white matter integrity between tracts in our stroke participants did not correlate with age ($r = 0.20$, $p = 0.42$). We believe this is because disruptions to white matter integrity due to stroke supersede those due to aging. This is supported by trends in our data between shared variance for the poststroke participants and chronicity ($r = 0.42$, $p = 0.07$) and lesion volume ($r = 0.41$, $p = 0.07$). Taken together, diminished integrity in both ipsilesional and contralesional hemispheres, and the large shared variance across the network in stroke participants, which is not correlated with age, suggest that there is a general stroke-related factor affecting the frontoparietal network white matter integrity. This finding has important implications for interpreting quantitative white matter studies in stroke. First, reporting diffusion metrics as a proportion of the same structure in the contralesional hemisphere may be biased by contralesional microstructural changes. Second, in light of network wide changes, single tract studies are at risk of over simplifying the relationship between white matter structure and behavior.

4.3. Tract integrity has a positive correlation with haptic performance

For the analysis of the relationship between haptic performance of the affected hand poststroke and integrity of individual tracts we prioritized ipsilesional and interhemispheric tracts because others have shown that areas of the most reduced structural connectivity are found in the ipsilesional hemisphere (Crofts et al., 2011), and the ipsilesional hemisphere would receive primary afferent input. In the poststroke participants a good relationship between ipsilesional thalamus-M1 integrity and haptic performance was identified. When thinking about the axons that travel between thalamus and M1 cortex it is tempting to assume the data reflect primarily efferent pathways. Of course, an important limitation of probabilistic tractography is the inability to distinguish between afferent and efferent tracts. One possible mechanism by which thalamus–M1 white matter integrity may support haptic performance is through facillatory drive to M1 from the dentate nucleus via the dentato-thalamo-cortical pathway. The dentate nucleus puts forth facilitation into the contralateral M1 through synaptic relay in the ventral lateral thalamus (Middleton and Strick, 2000; Dum et al., 2002); Ramnani, 2006). A second possible mechanism by which thalamus–M1 white matter may support haptic performance is through afferent input directly to M1. Some experiments have shown that the M1 hand area receives input from peripheral receptors (Friedman and Jones, 1981; Darian-Smith and Darian-Smith, 1993). There is still a question whether M1 receives direct afferents or only input through S1 (Reis et al., 2008).

Previous studies have related the integrity of the descending fibers from M1 to handgrip (Schulz et al., 2012), motor skill (Schaechter et al., 2009; Lindenberg et al., 2010), and potential for recovery (Stinear et al., 2007; Lindenberg et al., 2012; Newton et al., 2006; Werring et al., 2000). When the M1-peduncular tract, which includes the CST, is generated with diffusion tractography, at the level of the internal capsule, it is located in the posterior limb of the internal capsule (PLIC) between the posterior putamen and the thalamus (Newton et al.,

Table 5
Pearson's correlation of tract diffusion parameters by affected hand HASTe score.

	Mean FA		Mean MD		Mean AD		Mean RD	
	r	p-Value	r	p-Value	r	p-Value	r	p-Value
Affected HASTe								
Ipsilesional T–S1	0.18	0.498	−0.10	0.238	−0.33	0.207	−0.30	0.265
Ipsilesional T–M1	0.46	0.054	−0.62	0.006*	−0.56	0.163	−0.62	0.006*
Ipsilesional S1–MFG	0.29	0.259	−0.10	0.760	−0.03	0.888	−0.09	0.715
Ipsilesional S1–SII	0.49	0.047	−0.46	0.062	−0.37	0.138	−0.48	0.049
S1–S1	0.47	0.063	−0.42	0.106	−0.31	0.234	−0.42	0.101
Precuneus	0.18	0.510	−0.09	0.735	−0.11	0.673	−0.07	0.777

After Bonferroni correction p-values are considered significant at p ≤ 0.008, statistically significant correlations are indicated by an *.

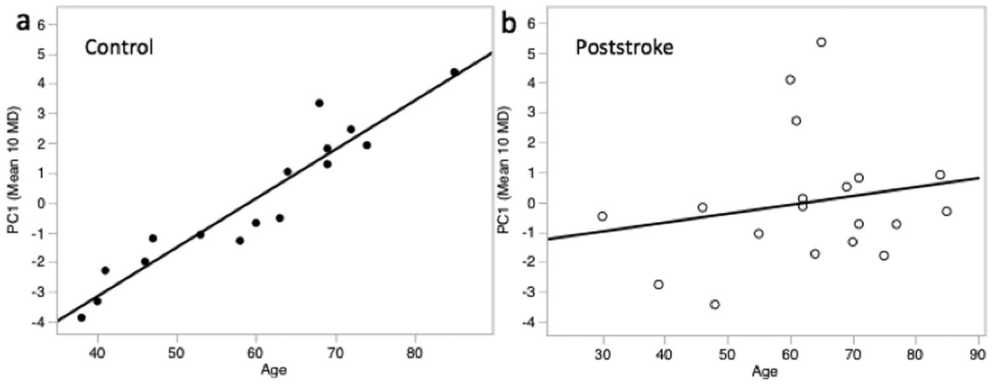

Fig. 4. Shared variance across 10 frontoparietal tract MD values correlates with age in control participants. The first principal component (PC1) accounting for the variance across tracts was strongly correlated with age in the control participants ($r = 0.95$, $p < 0.0001$) but not in the poststroke participants ($r = 0.20$, $p = 0.42$).

2006). Therefore, the CST is closely adjacent to the thalamus–M1 tract quantified here; it is possible there was overlap. Because haptic performance measured by the HASTe is a somatosensory task, which is in part dependent upon motor manipulation, we wished to discern whether the positive relationship between thalamus–M1 integrity and HASTe score was a function of better motor performance. In post-hoc analyses we found no relationship between motor performance, measured by the 6-item Wolf and thalamus–M1 integrity. Nor was there a relationship between 6-item Wolf scores and haptic performance. These findings support the idea of a unique role of thalamus–M1 integrity to haptic performance in chronic stroke.

The T–S1 tract integrity should reflect all afferent axons to the primary somatosensory cortex. In two participants, one with right and one with left hemisphere stroke we were unable to generate a T–S1 tract due to the lesion being within the tract. Both of these participants had HASTe scores so low they could have been attributed to chance (4/18 and 7/18). Given we did not find a correlation between poststroke ipsilesional T–S1 integrity and affected HASTe scores, and T–S1 was not retained in the regression model, it suggest T–S1 tract is necessary but not sufficient for good haptic performance.

Precuneus interhemispheric white matter integrity had the strongest relationship to haptic performance in the control participants. This finding echoes other studies in healthy adults, which relate precuneus function to sensory discrimination. Van de Winckel et al., found the precuneus was activated bilaterally in unfamiliar but not during familiar shape and length discrimination (Van de Winckel et al., 2012). Pellijeff and colleagues found precuneus activation related to the updating of limb posture (Pellijeff et al., 2006). When transcranial magnetic stimulation was used to inhibit the precuneus, impaired performance on grating orientation, a measure of tactile spatial acuity resulted (Zangaladze et al., 1999). The role of precuneus cortex in the sensorimotor transformations associated with goal directed movements, such as haptic exploration, is also the subject of a review (Cavanna and Trimble, 2006).

4.4. Frontoparietal network integrity predicts poststroke haptic performance

When a multivariate approach, which accounts for the influence of all variables, including age, was used to predict HASTe scores, 90% of the variability in affected hand scores poststroke and 87% of the variability in right hand scores in control participants could be attributed to network white matter integrity. Age was not a predictor in either model. The strongest predictor in both poststroke and control models was the precuneus interhemispheric tract. This finding is aligned with data from a previous study in which we found precuneus cortex fMRI activation correlated with HASTe scores in individuals with chronic left hemisphere stroke (Borstad et al., 2012b). Precuneus functional MRI activation has also been associated with length but not shape discrimination in a study of individuals with chronic left hemisphere subcortical stroke (Van de Winckel et al., 2012). In the broad context of the relationship between poststroke white matter integrity and sensory-motor behavior, this studies findings parallel a recent large study of acute stroke in which a large percentage of sensory-motor deficit was explained by white matter damage (Corbetta et al., 2015) and exemplify the idea that neurologic disorders are due to problems of network function (Stam, 2014).

A few limitations should be considered when interpreting this data. We used 32 diffusion-weighting gradient directions diffusion data, which may not be as robust to issues of complex intra-voxel fiber architecture and partial volume effects as acquisitions with a greater number of gradient directions or tensor-free approaches. It is possible that the high variability in FA found in our S1-SII tract is related to the tracts' smaller, peripheral, and more acute path (Heiervang et al., 2006), therefore we feel care should be taken in interpretation of S1-SII diffusion parameter values. The dense intra-cortical connections between S1 and M1 are known to be important to sensorimotor processes (see recent review by Borich) (Borich et al., 2015), however, they were not quantified in this study because accurate tracking in the network of horizontal intra-cortical white matter is a limitation of probabilistic tractography (Jbabdi and Johansen-Berg, 2011). They should be included in future efforts to quantify this network. Regardless of our efforts to check the position of each tract of interest in each participant, subtle misregistration between participant data and the standard space masks may have resulted in small differences in tracts generated and the diffusion metrics derived. By having an age matched control group and applying the same rigorous registration and analysis process across groups we attempted to mitigate this effect. Diffusion metrics may have been underestimated in poststroke participants as a minimum FA threshold of 0.2 was used to constrain probabilistic tracking. We chose conservative thresholding to reduce sensitivity to noise and partial volume effects making false positives less likely (Behrens et al., 2003). However, this may have resulted in smaller samples in degraded tracts (Johansen-Berg and Behrens, 2009). In spite of this we identified many differences in tract integrity between poststroke and control participants and statistically significant and plausible relationships with behavior, which lend support to our approach. The poststroke participants in this study had heterogeneous lesion locations. While lesions were masked to avoid contribution to registration error, the lack of strict anatomical criteria for lesions of the participants included here likely contributed to variability, decreasing the sensitivity of this study, however, variable lesion size and location is reflective of the clinical population with stroke and likely improves generalizability of our findings.

5. Conclusions

This study is contributes to the growing body of literature that seeks to use neuroimaging information to predict functional potential and to

target rehabilitation interventions (Riley et al., 2011; Gauthier et al., 2012; Stinear and Ward, 2013). We demonstrated the importance of frontoparietal white matter in mediating haptic performance and specifically identified that T–M1 and precuneus interhemispheric tracts may be appropriate targets for piloting rehabilitation interventions, such as noninvasive brain stimulation, when the goal is to improve haptic performance of the affected hand in chronic stroke. The relative strength of these findings is good given the sample was heterogeneous and moderately sized, and a reliable white matter quantification approach was employed. Future studies may increase power to identify neural correlates of poststroke sensorimotor performance by combining functional connectivity and tensor-free structural measurement into one analysis (Calamante et al., 2013).

Acknowledgments

This work was supported in part by a PODS I scholarship from the Foundation for Physical Therapy, Inc.; also The Ohio State University Neuroscience Signature Program and The OSU Center for Clinical and Translational Research award number TL RR025753 from the National Center for Research Resources, funded by the Office of the Director, National Institutes of Health and supported by the NIH Road map for Medical Research. The content is solely the responsibility of the authors and does not necessarily represent the official views of the National Center for Research Resources or the National Institutes of Health.

Appendix A. Supplementary data

Supplementary data to this article can be found online at http://dx.doi.org/10.1016/j.nicl.2015.11.007.

References

Andrews, R.J., 1991. Transhemispheric diaschisis. A review and comment. Stroke 22, 943–949.
Auriat, A., Borich, M., Snow, N., Wadden, K., Boyd, L., 2015. Comparing a diffusion tensor and non-tensor approach to white matter fiber tractography in chronic stroke. NeuroImage Clin. 7, 771–781.
Basser, P.J., Pierpaoli, C., 1996. Microstructural and physiological features of tissues elucidated by quantitative-diffusion-tensor MRI. J. Magn. Reson. B 111, 209–219.
Bazin, P.L., Cuzzocreo, J.L., Yassa, M.A., Gandler, W., McAuliffe, M.J., Bassett, S.S., Pham, D.L., 2007. Volumetric neuroimage analysis extensions for the MIPAV software package. J. Neurosci. Methods 165, 111–121.
Behrens, T.E.J., Johansen-Berg, H., Woolrich, M.W., Smith, S.M., Wheeler-Kingshott, C.A.M., Boulby, P.A., Barker, G.J., Sillery, E.L., Sheehan, K., Ciccarelli, O., 2003. Non-invasive mapping of connections between human thalamus and cortex using diffusion imaging. Nat. Neurosci. 6, 750–757.
Benjamini, Y., Hochberg, Y., 1995. Controlling the false discovery rate: a practical and powerful approach to multiple testing. J. R. Stat. Soc. Ser. B Methodol. 289–300.
Bogard, K., Wolf, S., Zhang, Q., Thompson, P., Morris, D., Nichols-Larsen, D., 2009. Can the Wolf Motor Function Test be streamlined? Neurorehabil. Neural Repair 23, 422–428.
Borich, M.R., Mang, C., Boyd, L.A., 2012. Both projection and commissural pathways are disrupted in individuals with chronic stroke: investigating microstructural white matter correlates of motor recovery. BMC Neurosci. 13, 107.
Borich, M., Brodie, S., Gray, W., Ionta, S., Boyd, L., 2015. Understanding the role of the primary somatosensory cortex: opportunities for rehabilitation. Neuropsychologia (in press).
Borstad, A., Schmalbrock, P., Choi, S., Nichols-Larsen, D.S., 2012a. Neural correlates supporting sensory discrimination after left hemisphere stroke. Brain Res. 1460, 78–87.
Borstad, A., Schmalbrock, P., Choi, S., Nichols-Larsen, D.S., 2012b. Neural correlates supporting sensory discrimination after left hemisphere stroke. Brain Res. 1460, 78–87.
Borstad, A., Altenburger, A., Hannigan, A., LaPorte, J., Mott, R., Nichols-Larsen, D.S., 2015. Design, fabrication, and administration of the Hand Active Sensation Test (HASTe). J. Vis. Exp. (103), e53178.
Buch, E.R., Shanechi, A.M., Fourkas, A.D., Weber, C., Birbaumer, N., Cohen, L.G., 2012. Parietofrontal integrity determines neural modulation associated with grasping imagery after stroke. Brain 135, 596–614.
Budde, M.D., Kim, J.H., Liang, H.F., Schmidt, R.E., Russell, J.H., Cross, A.H., Song, S.K., 2007. Toward accurate diagnosis of white matter pathology using diffusion tensor imaging. Magn. Reson. Med. 57, 688–695.
Calamante, F., Masterton, R.A., Tournier, J.-D., Smith, R.E., Willats, L., Raffelt, D., Connelly, A., 2013. Track-weighted functional connectivity (TW-FC): a tool for characterizing the structural–functional connections in the brain. NeuroImage 70, 199–210.
Carey, L.M., Matyas, T.A., 2011. Frequency of discriminative sensory loss in the hand after stroke in a rehabilitation setting. J. Rehabil. Med. 43, 257–263.
Carey, L.M., Abbott, D.F., Harvey, M.R., Puce, A., Seitz, R.J., Donnan, G.A., 2011. Relationship between touch impairment and brain activation after lesions of subcortical and cortical somatosensory regions. Neurorehabil. Neural Repair 25, 443–457.
Carter, A.R., Patel, K.R., Astafiev, S.V., Snyder, A.Z., Rengachary, J., Strube, M.J., Pope, A., Shimony, J.S., Lang, C.E., Shulman, G.L., 2012. Upstream dysfunction of somatomotor functional connectivity after corticospinal damage in stroke. Neurorehabil. Neural Repair 26, 7–19.
Cavanna, A.E., Trimble, M.R., 2006. The precuneus: a review of its functional anatomy and behavioural correlates. Brain 129, 564.
Choi, S., Cunningham, D.T., Aguila, F., Corrigan, J.D., Bogner, J., Mysiw, W.J., Knopp, M.V., Schmalbrock, P., 2011. DTI at 7 and 3 T: systematic comparison of SNR and its influence on quantitative metrics. Magn. Reson. Imaging 29, 739–751.
Classen, J., Steinfelder, B., Liepert, J., Stefan, K., Celnik, P., Cohen, L.G., Hess, A., Kunesch, E., Chen, R., Benecke, R., 2000. Cutaneomotor integration in humans is somatotopically organized at various levels of the nervous system and is task dependent. Exp. Brain Res. 130, 48–59.
Connell, L.A., Lincoln, N.B., Radford, K.A., 2008. Somatosensory impairment after stroke: frequency of different deficits and their recovery. Clin. Rehabil. 22, 758.
Corbetta, M., Ramsey, L., Callejas, A., Baldassarre, A., Hacker, C.D., Siegel, J.S., Astafiev, S.V., Rengachary, J., Zinn, K., Lang, C.E., 2015. Common behavioral clusters and subcortical anatomy in stroke. Neuron 85, 927–941.
Crofts, J.J., Higham, D.J., Bosnell, R., Jbabdi, S., Matthews, P.M., Behrens, T.E.J., Johansen-Berg, H., 2011. Network analysis detects changes in the contralesional hemisphere following stroke. NeuroImage 54, 161–169.
Darian-Smith, C., Darian-Smith, I., 1993. Thalamic projections to areas 3a, 3b, and 4 in the sensorimotor cortex of the mature and infant macaque monkey. J. Comp. Neurol. 335, 173–199.
De Weijer, A.D., Mandl, R.C.W., Sommer, I.E.C., Vink, M., Kahn, R.S., Neggers, S.F.W., 2010. Human fronto-tectal and fronto-striatal-tectal pathways activate differently during anti-saccades. Front. Hum. Neurosci. 4.
Dum, R.P., Li, C., Strick, P.L., 2002. Motor and nonmotor domains in the monkey dentate. Ann. N. Y. Acad. Sci. 978, 289–301.
Friedman, D., Jones, E., 1981. Thalamic input to areas 3a and 2 in monkeys. J. Neurophysiol. 45, 59–85.
Gaubert, C., Mockett, S., 2000. Inter-rater reliability of the Nottingham method of stereognosis assessment. Clin. Rehabil. 14, 153–159.
Gauthier, L.V., Taub, E., Mark, V.W., Barghi, A., Uswatte, G., 2012. Atrophy of spared gray matter tissue predicts poorer motor recovery and rehabilitation response in chronic stroke. Stroke 43, 453–457.
Harada, T., Saito, D.N., Kashikura, K.I., Sato, T., Yonekura, Y., Honda, M., Sadato, N., 2004. Asymmetrical neural substrates of tactile discrimination in humans: a functional magnetic resonance imaging study. J. Neurosci. 24, 7524.
Heiervang, E., Behrens, T.E.J., Mackay, C.E., Robson, M.D., Johansen-Berg, H., 2006. Between session reproducibility and between subject variability of diffusion MR and tractography measures. NeuroImage 33, 867–877.
Jbabdi, S., Johansen-Berg, H., 2011. Tractography: where do we go from here? Brain Connect. 1, 169–183.
Jenkinson, M., Smith, S., 2001. A global optimisation method for robust affine registration of brain images. Med. Image Anal. 5, 143–156.
Jenkinson, M., Bannister, P., Brady, M., Smith, S., 2002. Improved optimization for the robust and accurate linear registration and motion correction of brain images. NeuroImage 17, 825–841.
Johansen-Berg, H., Behrens, T.E.J., 2009. Diffusion MRI. Academic Press, London.
Kim, J.S., Choi-Kwon, S., 1996. Discriminative sensory dysfunction after unilateral stroke. Stroke 27, 677.
Kohama, S.G., Rosene, D.L., Sherman, L.S., 2012. Age-related changes in human and non-human primate white matter: from myelination disturbances to cognitive decline. Age 34, 1093–1110.
Lederman, S.J., Klatzky, R.L., 1997. Haptic aspects of motor control. Handbook of Neuropsychology 11, 131–148.
Lederman, S.J., Klatzky, R.L., 1998. The hand as a perceptual system. Clin. Dev. Med. 16–35.
Lim, D.H., Mohajerani, M.H., LeDue, J., Boyd, J., Chen, S., Murphy, T.H., 2012. In vivo large-scale cortical mapping using channelrhodopsin-2 stimulation in transgenic mice reveals asymmetric and reciprocal relationships between cortical areas. Front. Neural Circ. 6.
Lindberg, P.G., Skejø, P.H., Rounis, E., Nagy, Z., Schmitz, C., Wernegren, H., Bring, A., Engardt, M., Forssberg, H., Borg, J., 2007. Wallerian degeneration of the corticofugal tracts in chronic stroke: a pilot study relating diffusion tensor imaging, transcranial magnetic stimulation, and hand function. Neurorehabil. Neural Repair 21 (6), 551–560.
Lindberg, P.G., Bensmail, D., Bussel, B., Maier, M.A., Feydy, A., 2011. Wallerian degeneration in lateral cervical spinal cord detected with diffusion tensor imaging in four chronic stroke patients. J. Neuroimaging 21, 44–48.
Lindenberg, R., Renga, V., Zhu, L., Betzler, F., Alsop, D., Schlaug, G., 2010. Structural integrity of corticospinal motor fibers predicts motor impairment in chronic stroke. Neurology 74, 280–287.
Lindenberg, R., Zhu, L.L., Rüber, T., Schlaug, G., 2012. Predicting functional motor potential in chronic stroke patients using diffusion tensor imaging. Hum. Brain Mapp. 33, 1040–1051.
Middleton, F.A., Strick, P.L., 2000. Basal ganglia and cerebellar loops: motor and cognitive circuits. Brain Res. Rev. 31, 236–250.
Newton, J.M., Ward, N.S., Parker, G.J.M., Deichmann, R., Alexander, D.C., Friston, K.J., Frackowiak, R.S.J., 2006. Non-invasive mapping of corticofugal fibres from multiple motor areas—relevance to stroke recovery. Brain 129, 1844.
Oldfield, R.C., 1971. The assessment and analysis of handedness: the Edinburgh inventory. Neuropsychologia 9, 97–113.

Orrison, W.W., 2008. Atlas of Brain Function. Thieme Medical Pub.
Pellijeff, A., Bonilha, L., Morgan, P.S., McKenzie, K., Jackson, S.R., 2006. Parietal updating of limb posture: an event-related fMRI study. Neuropsychologia 44, 2685–2690.
Pierpaoli, C., Alger, J.R., Righini, A., Mattiello, J., Dickerson, R., Des Pres, D., Barnett, A., Di Chiro, G., 1996. High temporal resolution diffusion MRI of global cerebral ischemia and reperfusion. J. Cereb. Blood Flow Metab. 16, 892–905.
Ramnani, N., 2006. The primate cortico-cerebellar system: anatomy and function. Nat. Rev. Neurosci. 7, 511–522.
Reis, J., Swayne, O.B., Vandermeeren, Y., Camus, M., Dimyan, M.A., Harris-Love, M., Perez, M.A., Ragert, P., Rothwell, J.C., Cohen, L.G., 2008. Contribution of transcranial magnetic stimulation to the understanding of cortical mechanisms involved in motor control. J. Physiol. 586, 325–351.
Riley, J.D., Le, V., Der-Yeghiaian, L., See, J., Newton, J.M., Ward, N.S., Cramer, S.C., 2011. Anatomy of stroke injury predicts gains from therapy. Stroke 42, 421–426.
Rorden, C., Brett, M., 2000. Stereotaxic display of brain lesions. Behav. Neurol. 12, 191–200.
Salat, D., Tuch, D., Greve, D., Van Der Kouwe, A., Hevelone, N., Zaleta, A., Rosen, B., Fischl, B., Corkin, S., Rosas, H.D., 2005. Age-related alterations in white matter microstructure measured by diffusion tensor imaging. Neurobiol. Aging 26, 1215–1227.
Schaechter, J.D., Fricker, Z.P., Perdue, K.L., Helmer, K.G., Vangel, M.G., Greve, D.N., Makris, N., 2009. Microstructural status of ipsilesional and contralesional corticospinal tract correlates with motor skill in chronic stroke patients. Hum. Brain Mapp. 30, 3461–3474.
Schlaug, G., Siewert, B., Benfield, A., Edelman, R.R., Warach, S., 1997. Time course of the apparent diffusion coefficient (ADC) abnormality in human stroke. Neurology 49, 113–119.
Schulz, R., Park, C.H., Boudrias, M.H., Gerloff, C., Hummel, F.C., Ward, N.S., 2012. Assessing the integrity of corticospinal pathways from primary and secondary cortical motor areas after stroke. Stroke 43, 2248–2251.
Seidl, A., 2014. Regulation of conduction time along axons. Neuroscience 276, 126–134.
Smith, S.M., 2002. Fast robust automated brain extraction. Hum. Brain Mapp. 17, 143–155.
Smith, S.M., De Stefano, N., Jenkinson, M., Matthews, P.M., 2001. Normalized accurate measurement of longitudinal brain change. J. Comput. Assist. Tomogr. 25, 466.
Smith, S.M., Zhang, Y., Jenkinson, M., Chen, J., Matthews, P.M., Federico, A., De, S.N., 2002. Accurate, robust, and automated longitudinal and cross-sectional brain change analysis. NeuroImage 17, 479–489.
Smith, S.M., Jenkinson, M., Woolrich, M.W., Beckmann, C.F., Behrens, T.E., Johansen-Berg, H., Bannister, P.R., De, L.M., Drobnjak, I., Flitney, D.E., Niazy, R.K., Saunders, J., Vickers, J., Zhang, Y., De, S.N., Brady, J.M., Matthews, P.M., 2004. Advances in functional and structural MR image analysis and implementation as FSL. NeuroImage 23 (Suppl. 1), S208–S219.
Song, S.K., Sun, S.W., Ju, W.K., Lin, S.J., Cross, A.H., Neufeld, A.H., 2003. Diffusion tensor imaging detects and differentiates axon and myelin degeneration in mouse optic nerve after retinal ischemia. NeuroImage 20, 1714–1722.
Stam, C.J., 2014. Modern network science of neurological disorders. Nat. Rev. Neurosci. 15, 683–695.
Stinear, C.M., Ward, N.S., 2013. How useful is imaging in predicting outcomes in stroke rehabilitation? Int. J. Stroke 8, 33–37.
Stinear, C.M., Barber, P.A., Smale, P.R., Coxon, J.P., Fleming, M.K., Byblow, W.D., 2007. Functional potential in chronic stroke patients depends on corticospinal tract integrity. Brain 130, 170–180.
Stoeckel, M.C., Weder, B., Binkofski, F., Buccino, G., Shah, N.J., Seitz, R.J., 2003. A fronto-parietal circuit for tactile object discrimination: an event-related fMRI study. NeuroImage 19, 1103–1114.
Tunik, E., Rice, N.J., Hamilton, A., Grafton, S.T., 2007. Beyond grasping: representation of action in human anterior intraparietal sulcus. NeuroImage 36, T77–T86.
Van de Winckel, A., Sunaert, S., Wenderoth, N., Peeters, R., Van Hecke, P., Feys, H., Horemans, E., Marchal, G., Swinnen, S.P., Perfetti, C., 2005. Passive somatosensory discrimination tasks in healthy volunteers: differential networks involved in familiar versus unfamiliar shape and length discrimination. NeuroImage 26, 441–453.
Van de Winckel, A., Wenderoth, N., De Weerdt, W., Sunaert, S., Peeters, R., Van Hecke, W., Thijs, V., Swinnen, S.P., Perfetti, C., Feys, H., 2012. Frontoparietal involvement in passively guided shape and length discrimination: a comparison between subcortical stroke patients and healthy controls. Exp. Brain Res. 220, 179–189.
Vos, S.B., Jones, D.K., Jeurissen, B., Viergever, M.A., Leemans, A., 2012. The influence of complex white matter architecture on the mean diffusivity in diffusion tensor MRI of the human brain. NeuroImage 59, 2208–2216.
Wakana, S., Jiang, H., Nagae-Poetscher, L.M., van Zijl, P., Mori, S., 2004. Fiber tract-based atlas of human white matter anatomy. Radiology 230, 77.
Werring, D.J., Toosy, A.T., Clark, C.A., Parker, G.J.M., Barker, G.J., Miller, D.H., Thompson, A.J., 2000. Diffusion tensor imaging can detect and quantify corticospinal tract degeneration after stroke. J. Neurol. Neurosurg. Psychiatry 69, 269–272.
Williams, P.S., Basso, D.M., Case-Smith, J., Nichols-Larsen, D.S., 2006. Development of the Hand Active Sensation Test: reliability and validity. Arch. Phys. Med. Rehabil. 87, 1471–1477.
Yang, D.S., Hong, J.H., Byun, W.M., Kwak, S.Y., Ahn, S.H., Lee, H., Hwang, C.H., Jang, S.H., 2009. Identification of the medial lemniscus in the human brain: combined study of functional MRI and diffusion tensor tractography. Neurosci. Lett. 459, 19–24.
Yin, D., Yan, X., Fan, M., Hu, Y., Men, W., Sun, L., Song, F., 2013. Secondary degeneration detected by combining voxel-based morphometry and tract-based spatial statistics in subcortical strokes with different outcomes in hand function. Am. J. Neuroradiol. 34, 1341–1347.
Zangaladze, A., Epstein, C.M., Grafton, S.T., Sathian, K., 1999. Involvement of visual cortex in tactile discrimination of orientation. Nature 401, 587–590.
Zhang, Y., Brady, M., Smith, S., 2001. Segmentation of brain MR images through a hidden Markov random field model and the expectation–maximization algorithm. Med. Imaging IEEE Trans. 20, 45–57.